

## ***Interactive comment on “The ICON-1.2 hydrostatic atmospheric dynamical core on triangular grids – Part 1: Formulation and performance of the baseline version” by H. Wan et al.***

H. Wan et al.

hui.wan@zmaw.de

Received and published: 19 April 2013

We thank Dr. Gassmann for her comments and suggestions which are helpful for revising the manuscript. Our reply is given below.

### **1) Equivalent resolution (Table 2 and discussion on page 83)**

**The ‘by eye comparison’ to ECHAM is not an objective scientific method. It is very easy to give the effective degrees of freedom or in other words the total number of effective number of mass points for ICON in comparison to ECHAM.**

**In the triangular C-grid one has 3 normal velocity components where a compara-**

Full Screen / Esc

Printer-friendly Version

Interactive Discussion

Discussion Paper



ble quadrilateral mesh has 2 normal velocity components. The work by Thurner (2008) showed how the third degree of freedom is slaved to account for a linear dependence among the three velocity components on a hexagonal grid. Whatever one is doing – either go to the hexagonal C-grid where the overspecification can be treated without disrupting wave propagation – or stay with the triangular C-grid and apply some unphysical filtering as it is done in the present model description – eventually the third degree of freedom does not provide any new dynamical information. Therefore we have to conclude that a hexagon – which contains 3 normal components  $\Rightarrow$  effectively 2 normal components – is comparable to a quadrilateral grid box. Hence we have to count the number of hexagons (=half of the number of triangles) to find the effective number of mass points. Interestingly, comparing the  $n_m$  for ICON and ECHAM in table 2, we find approximately that  $n_m$  for ECHAM is about half the number of triangles (the  $n_m$  for ICON). The reason why the ratio is not exactly met and there are less  $n_m$  for ICON than expected from this consideration is related to the fact that in a triangular C-grid model, the tracer advection (in this case the temperature advection) is performed a bit more precisely. This increases the overall accuracy as can be observed by similar examples that are known from Skamarock and Gassmann (2011) when they are increasing the order of accuracy of the tracer advection in the baroclinic wave test.

Firstly we clarify that the equivalent resolutions we attempt to establish between the ICOHDC and the spectral transform dynamical core of ECHAM are the resolutions that produce the same solution quality.

Dr. Gassmann's reasoning above regarding the effective number of Degrees Of Freedom (DOF) focuses on the relative DOF in the mass and velocity fields. Although this issue is important and is directly related to the existence of computational modes in the discrete dispersion relation, such a DOF, just like the total DOF, does not provide information about the order of accuracy of the whole suite of discretizations applied

[Full Screen / Esc](#)[Printer-friendly Version](#)[Interactive Discussion](#)[Discussion Paper](#)

to the nonlinear governing equations, nor about the impact of other components such as the form and magnitude of numerical diffusion. The latter two aspects are, in our opinion, as important as the dispersion relation in determining the properties (hence the quality) of the numerical solution. Because the ICOHDC and the spectral core of ECHAM are based on different discretization concepts (low-order finite-difference versus spectral transform), and employ different values of the hyper-diffusion coefficient, we believe the equivalent resolutions can not be easily estimated a priori, but need to be identified by evaluating results from numerical experiments.

If Dr. Gassmann's conclusion of 1:1 mass point ratio between hexagonal-C and quadrilateral grids were valid regardless of the discretization scheme applied on the quadrilateral grid, it would follow that any two models built on quadrilateral grids would have the same equivalent resolution when the number of mass points are equal. However, in the work of Williamson (2008a), it was concluded from aqua-planet simulations that ( $2^\circ$ , T42), ( $1^\circ$ , T85) and ( $0.5^\circ$ , T170) were equivalent resolution pairs between the NCAR finite volume and spectral transform dynamical cores. Although both models use latitude-longitude (i.e., quadrilateral) grids, and the physics parameterizations, which are computed at the mass points, are expected to play an important role in the simulations, the ratio of mass points in these equivalent pairs are approximately 1.6:1 (FV vs. spectral), not 1:1.

In the manuscript we made the comment that between the equivalent resolutions identified by comparing results of the baroclinic wave test (Table 2), the average grid spacing of the triangular grid matches the zonal grid size at  $60^\circ\text{N}$  on the Gauss grid of the corresponding spectral resolution. One might consider comparing grid spacing as equivalent to comparing the number of mass points. It is worth noting that (i) this match is observed under the condition that both models employ similar finite-difference discretizations for the nonlinear terms in the governing equations, and (ii) the match means that near  $60^\circ\text{N}$  the ratio of mass count is about 1:1, not 2:1 (ICOHDC vs. ECHAM) as suggested by Dr. Gassmann.

To summarize, we consider the equivalent resolutions as a concept to compare the quality of numerical solutions provided by different models. The effective mass DOF proposed by Dr. Gassmann is most relevant to the dispersion relation, but does not reflect differences in discretization concepts (e.g., low-order finite-difference versus spectral transform), the resulting differences in the order of accuracy, and the impact of numerical diffusion. The effective mass DOF can therefore not be used in a straightforward way to estimate a priori the equivalent resolutions between the ICOHDC and ECHAM.

Furthermore, we remark that temperature advection in the present ICOHDC is calculated using Eq. (26) of the discussion paper, in which the mass and heat fluxes at triangle edges are computed by first averaging the layer thickness and temperature from cell centers to edge midpoints using a distance-based linear interpolation and then multiplying by the normal velocity. Because of the rather simple flux calculation and the inherent property of the divergence operator, the horizontal temperature advection is only first-order accurate. Higher-order transport algorithms are *not* yet used for temperature in simulations presented in the paper. Therefore this important part of the model is *less* accurate than the counterpart in the spectral core. Clarifications regarding this point have been added to Sections 5.5, 5.11 and 6.1.2 of the revised manuscript.

Reference:

Williamson, D. L.: Equivalent finite volume and Eulerian spectral transform horizontal resolutions established from aqua-planet simulations, *Tellus A*, 60, 839–847, 2008a

**For the same dynamical resolution than a comparable quadrilateral mesh one needs thus approximately twice the number of mass points. One has to discuss what this means for the efficiency of an operational model where the computing time spent in physical parameterizations is dominating the overall timings. One could half the number of parameterization calls when using a hexagonal mesh.**

[Full Screen / Esc](#)[Printer-friendly Version](#)[Interactive Discussion](#)[Discussion Paper](#)

The goal of the present paper is to assess the ability of a specific triangular mesh discretization to reproduce important features of the large scale adiabatic and diabatically forced circulation, rather than to compare it to the hexagonal mesh variant in terms of accuracy or efficiency. Therefore, no conclusions are included in the paper on the relative merits of triangular and hexagonal mesh discretizations with respect to accuracy or efficiency. However, concerning the issue raised by Dr. Gassmann, it should be remarked that in real NWP and climate applications, various measures, for instance lower spatial resolution and calling frequencies, are commonly employed to reduce the computational cost of the model physics. Along this line, a triangular mesh allows for calculating, for example, radiative transfer which is by far the most expensive physics parameterization, at a reduced resolution (e.g. one grid level coarser) in a pretty straightforward way, reducing the computational cost by a factor of 4. For a hexagonal grid, it would be far less obvious how to use a reduced grid for particularly expensive physics parameterizations. In the revised paper we have added some discussion on this topic in the Introduction section.

## 2) Motivation for ICON

**I know that the main motivation for keeping the triangular C-grid mesh is the fact that grid refinement is based on the philosophy of dividing triangles in contrast to the grid stretching philosophy advocated in MPAS. The grid refinement issue is not discussed in this paper, but it needs at least to be mentioned as a motivation in the introduction. Why the MPAS approach is ruled out for ICON?**

We appreciate Dr. Gassmann's remark about the lack of references to the grid refinement capability, which is discussed in the introduction section of the revised paper among the motivations for the presented approach. The authors believe that the flexibility resulting from being able to perform local mesh refinement with triangular overlapping control volumes is an important advantage of discretizations approaches based on the triangular mesh. As described above, computationally expensive parameterizations could be run on coarser meshes, while on the other hand orographic features

[Full Screen / Esc](#)[Printer-friendly Version](#)[Interactive Discussion](#)[Discussion Paper](#)

could be described in much more detail and with greater precision, and physically important boundary fluxes and soil properties could be computed on a finer mesh and then exactly summed up onto a coarser one used by the other model components.

The present paper, as remarked previously, simply contains a description and assessment of the triangular mesh capabilities as carried out up to now for the hydrostatic version of the ICON dynamical core. Therefore, the paper does not aim at proposing a choice of one discretization approach over another. Rather, it aims at providing the basis for a discussion on these issues.

### 3) Aqua planet experiments

**I do not understand why two different vertical resolutions and two different time steps are used for ECHAM and ICON. One could learn more if using the same settings for the two models, especially as they employ exactly the same parameterizations.**

The aqua-planet experiments presented in the discussion paper were performed with the default configuration of ECHAM6 as used in its CMIP5 simulations, and with the resolution of ICOHAM as routinely used in the model development. The time steps used by the two models were different yet rather similar. The L31 vertical grid of ICOHAM and the L47 grid of ECHAM6 were identical in the troposphere (from the Earth's surface to 100 hPa). We therefore do not expect the zonal mean rain rates and the wave spectra of tropical precipitation shown in the paper to change significantly due to the time step and vertical resolution differences between the two models.

Nevertheless, in response to Dr. Gassmann's comment, we have re-run the simulations with the ECHAM6 model using the L31 grid and 8 min time step to allow for a cleaner comparison. Fig. 1 below compares the wavenumber-frequency diagrams (the raw spectra) of tropical precipitation in the T63L47-10min (left column) and T63L31-8min (right column) simulations. The results are indeed very similar in terms of both the characteristic pattern and the magnitude of the power. The statements we made about

Full Screen / Esc

Printer-friendly Version

Interactive Discussion

Discussion Paper



the ICOHAM-ECHAM intercomparison in Section 7 of the manuscript stay unchanged. In the revised manuscript, following Dr. Gassmann's suggestion, the T63L31-8min results of the ECHAM6 model are presented.

**It is not clear why ICON is showing less high frequency activity than ECHAM in Figures 15 and C1.**

Compared to Fig. 4 of Williamson (2008a) which shows the power spectra in two versions of the NCAR CAM model at various resolutions, and Fig. 4.91 of the APE Atlas (Williamson et al., 2011) which shows results from a number of models, the differences between the ICOHAM and ECHAM results are rather small. Given the fact that the wave spectrum, which indicates statistical features of the model "climate", has its own variability thus uncertainty, we can not yet conclude at this point whether the spectra in ECHAM and ICOHAM are significantly different.

The power of the tropical precipitation spectrum in APE has been shown to be sensitive to horizontal resolution (e.g., Williamson, 2008a, b). One can speculate that numerical diffusion plays a role as well. A comprehensive convergence analysis, like the work of Williamson (2008a, b), would provide valuable information on the comparison between ICOHAM and ECHAM. As mentioned in the paper, we have not yet performed the resolution sensitivity study mainly because of the practical need for tuning multiple empirical parameters in the physics package to make sure that both models produces reasonable real-world atmospheric simulations at multiple resolutions. Such a study is planned, and will be reported in a separate paper.

References:

Williamson, D. L.: Equivalent finite volume and Eulerian spectral transform horizontal resolutions established from aqua-planet simulations, *Tellus A*, 60, 839–847, 2008a

Williamson, D. L.: Convergence of aqua-planet simulations with increasing resolution in the Community Atmospheric Model, Version 3, *Tellus* (2008), 60A, 848–862, 2008b

Full Screen / Esc

Printer-friendly Version

Interactive Discussion

Discussion Paper



**4) Kinetic energy spectra** Since the paper discusses some unusual and unphysical momentum diffusion terms and we know that the diffusion is the main driver for the shape of a kinetic energy spectrum it would be interesting to discuss kinetic energy spectra for ECHAM and for ICON for either the Held-Suarez test or the aqua planet experiments.

Due to the relatively strong numerical diffusion in the ICON hydrostatic dynamical core, we expect the high-frequency end of the kinetic energy (KE) spectrum to drop faster and have less energy than in the spectral model ECHAM in the aqua-planet simulations shown in the discussion paper. The 250 hPa KE spectra (Fig. 2 below) indeed show such features. KE spectra of other models in APE or real-world climate simulations can be found in the work of, e.g., Williamson (2008b, NCAR spectral model), Lauritzen et al. (2012, NCAR finite volume model), Evans et al. (2012, NCAR spectral element model) and Rauscher et al. (2012, MPAS model). The spectrum in ECHAM generally follows the  $n^{-3}$  slope from wavenumber 10 up to the truncation limit, as a result of empirical tuning of the order and damping time scale of the hyper-diffusion. The spectrum in ICOHAM starts to deviate from the  $n^{-3}$  slope at about wavenumber 20, qualitatively similar to the behavior of the NCAR finite volume model at  $1.9 \times 2.5$  degree resolution as shown in Lauritzen et al. (2012). If we follow Skamarock (2011) and define the effective resolution of the triangular model as the point at which the slope of the simulated spectrum becomes steeper than  $n^{-3}$ , then the ICOHAM R2B4 APE simulation has a effective resolution of about 1000 km, translating to  $7\Delta x$  where  $\Delta x$  is the grid spacing, which seems to fall into the typical range of  $6\Delta x$  to  $10\Delta x$  pointed out by Skamarock (2011) for models that use G-grid discretization.

In recent years, dynamical core developers have been paying more attention to their models' ability to produce the observed transition of the KE spectrum from a  $n^{-3}$  slope in the inertial regime to a  $n^{-5/3}$  slope in the mesoscale regime, occurring at spatial

Full Screen / Esc

Printer-friendly Version

Interactive Discussion

Discussion Paper





scales of a few hundred kilometers (Nastrom and Gage 1985; Lindborg 1999). For example, Evans et al. (2012) showed that the CAM4 spectral element dynamical core, which uses 4th order hyper-viscosity, is able to resolve the transition when the horizontal resolution is increased to  $0.125^\circ$ . They pointed out that the CAM finite volume dynamical core with 2nd order divergence damping has a clearly weaker divergent component of the simulated flow, and expected the version with 4th order damping to behave similarly to the spectral element core. Takahashi et al. (2006) carried out a series of simulations with the spectral model AFES to empirically determine the appropriate relationship between the magnitude of hyper-diffusion and model resolution, aiming at correctly capturing the shape of the KE in both the inertial regime and the mesoscale regime. Their results suggest a scaling of  $n_0^{-3.22}$  (or  $\Delta x^{3.22}$ , where  $n_0$  is the truncation wavenumber, and  $\Delta x$  the grid spacing) for the diffusion coefficient. In the ICOHDC, the choice of a 4th order diffusion with damping time equal to time step implies a scaling of  $\Delta x^3$  according to Eq. (20) of the discussion paper, close to what is obtained by Takahashi et al. (2006). On the other hand, in terms of the absolute magnitude at each particular resolution, the diffusion in the ICOHDC/ICOHAM is considerably stronger than typically seen in climate models. The question is whether ICOHAM can produce the KE transition when the grid spacing is decreased, and if so, what is the critical grid size. This remains to be answered by high-resolution simulations in the future.

Fig. 2 and the discussion above are added to the revised manuscript.

#### References:

Evans, K. J., P. H. Lauritzen, S. K. Mishra, R. B. Neale, M. A. Taylor, J. J. Tribbia: AMIP Simulation with the CAM4 Spectral Element Dynamical Core. *J. Climate*, 26, 689–709, 2013

Lauritzen, P. H., Mirin, A. A, Truesdalea, J., Raeder, K., Andersonc, J. L., Bacmeistera, J. and Neale, R. B.: Implementation of new diffusion/filtering operators in the CAM-FV

[Full Screen / Esc](#)[Printer-friendly Version](#)[Interactive Discussion](#)[Discussion Paper](#)

dynamical core, *International Journal of High Performance Computing Applications*, 26, 63–73, 2012

Lindborg, E.: Can the atmospheric kinetic energy spectrum be explained by two-dimensional turbulence, *J. Fluid Mech.*, 388, 259–288, 1999

Nastrom, G., and K. S. Gage: A climatology of atmospheric wavenumber spectra of wind and temperature observed by commercial aircraft. *J. Atmos. Sci.*, 42, 950–960, 1985

Rauscher, S., T. Ringler, W. Skamarock, and A. Mirin: Exploring a Global Multi-Resolution Modeling Approach Using Aquaplanet Simulations. *J. Climate*, in press, 2012

Takahashi, Y. O., K. Hamilton, and W. Ohfuchi, Explicit global simulation of the mesoscale spectrum of atmospheric motions, *Geophys. Res. Lett.*, 33, L12812, 2006

**Fig. 1.** Comparison of the wavenumber-frequency diagrams of tropical precipitation (meridionally averaged between 10S and 10N) in aqua-planet simulations performed with the ECHAM6 model at T63L47 resolution with 600-second time step (left column) and at T63L31 resolution with 480-second time step (right column). The color shading shows the logarithm of the power of the symmetric component of the unnormalized spectra, diagnosed using the methodology of Wheeler and Kiladis (1999). The upper row shows results corresponding to the “Control” SST profile. The lower row corresponds to the “Qobs” profile.

**Fig. 2.** 250 hPa kinetic energy spectra in the aqua-planet simulations performed with ICOHAM at R2B4L31 resolution and with ECHAM6 at T63L31. The left panel corresponds to the “Control” SST profile, and the right panel the “Qobs” case. The spectra are diagnosed from daily output of instantaneous vorticity and divergence fields. Each curve shown in the figure is an average of 800 snapshots.

Interactive comment on *Geosci. Model Dev. Discuss.*, 6, 59, 2013.

C371

**GMDD**

6, C362–C373, 2013

Interactive  
Comment

Full Screen / Esc

Printer-friendly Version

Interactive Discussion

Discussion Paper



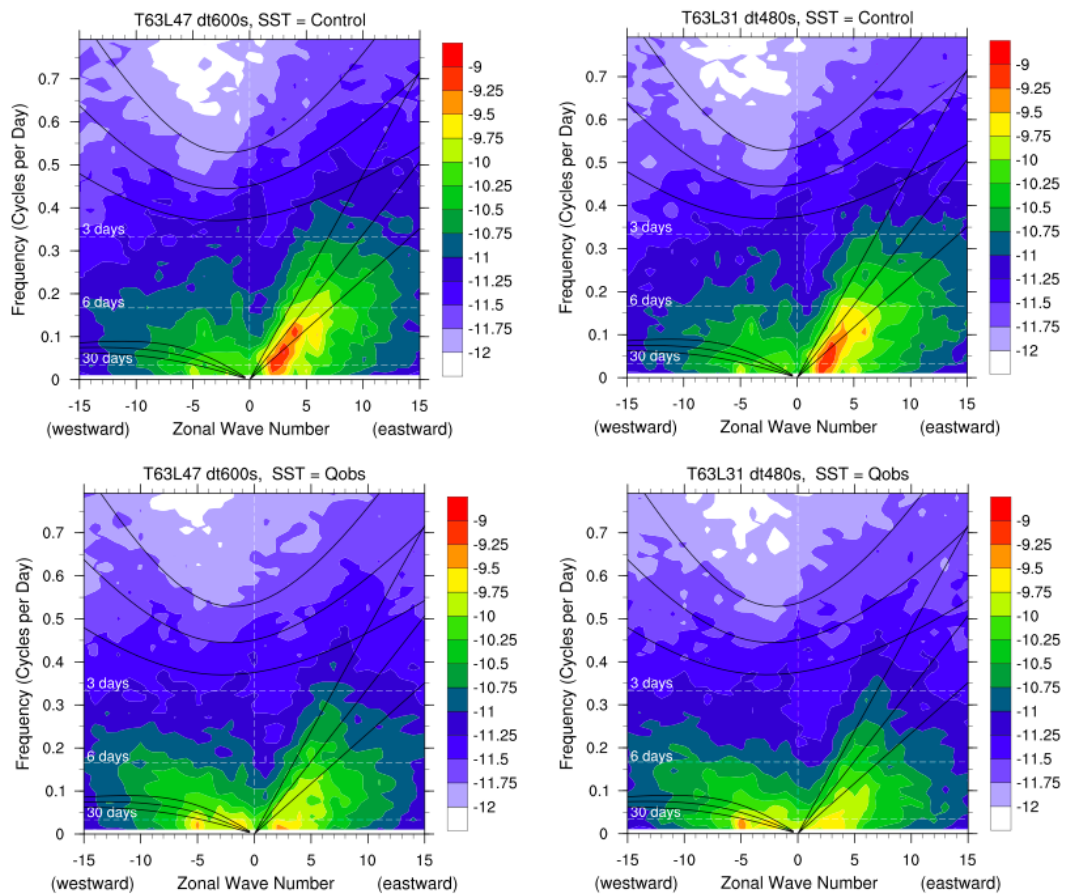


Fig. 1. Wavenumber-frequency diagrams of tropical precipitation

[Full Screen / Esc](#)[Printer-friendly Version](#)[Interactive Discussion](#)[Discussion Paper](#)

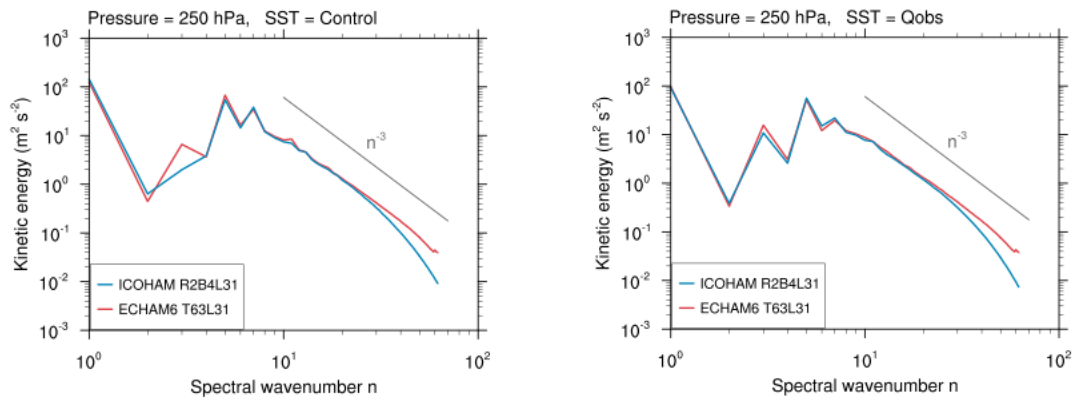


Fig. 2. 250 hPa kinetic energy spectra

Full Screen / Esc

Printer-friendly Version

Interactive Discussion

Discussion Paper